

Noise Free Detectors - Including wave front sensors !

Peter Moore – Isaac Newton Group – August 1999.

Updated - February 2001.

Updated - April 2001.

SUMMARY

An analysis of the degradation caused by electronic noise contamination in astronomic observations using charge-coupled devices is presented. From this, a technique for removing the electronic noise component from such observations is developed such that the SNR of observational measurement is improved. In addition the technique provides for increased dynamic range, reduced sensitivity of the electronics to temperature effects, and de-couples electronic conversion gain from readout speed.

1. INTRODUCTION

Given the extensive use of charge-coupled devices (CCDs) to detect photons in astronomy, the limitations of these devices still prevail to limit the science that can be obtained from them. The criteria of any planned observation must take into account the instrumental limitations to enable sufficient signal to be derived for the measurement accuracy required. In specific areas of investigation, for example time resolution photometry and faint object spectroscopy, observations are compromised by a lack of strong signal that, when coupled to the limitations of the overall instrument throughput, make observation or interpretation impossible. In instrumentation for astronomy, two characteristics of CCD detectors and readout electronics contribute directly to the available SNR of any observation. These are the quantum efficiency of the detector at the desired wavelength $Q?$ and the electronic or 'readout' noise Nrd associated with processing of the photon generated signal from the detector. Considering these two characteristics of the CCD a model of expected SNR S can be derived given the incoming photon flux from the object of interest I , the photon flux from background sky B , the time of integration t , and the number of pixels illuminated by the object of interest n . Thus the SNR is given by

$$S? = Q? It / [Q?(I + B)t + nNrd^2]^{1/2} \quad (1)$$

The contribution that readout noise plays in SNR can be seen by plotting the relative SNR for three observational scenarios. These are plotted in the attached figures with SNR shown as a function of seeing (fig 1), as a function of integration time (fig 2), and as a function of object photon flux (fig 3).

From these illustrations it is seen that readout noise plays a significant role in the determination of observation SNR under all conditions. Under marginal conditions, noise free observing has particular advantage in improving observation quality. In such cases noise free observing could make the difference between success and failure of the science objectives. However, it is to be noted that all observations will benefit productively from noise free

observing because, as readout noise is independent of the observed photon flux, readout noise sets the lower threshold of detection for the instrument.

2. DEFINING NOISE

Fig 4 shows a typical CCD based signal processing chain and defines the types of noise present and their origin within the signal processing chain. These noise types can be broadly classified into 3 classes described by their origin. Intrinsic noise sources are those generated by the process of detecting and conditioning the expected signal. Examples of this class are dark current, 1/f noise, quantization error, etc. The second class include sources of noise that are man made and influence the detection process by their proximity without actually taking part in the process itself, for example EMI. The third class is those sources generated by natural causes, for example, cosmic rays, sky brightness, lightning, etc. Fig.4 illustrates these sources. It is customary to specify all noise sources in units of equivalent signal (electrons) referenced to the detector.

PRNU, dark current, and fixed pattern noise are intrinsic noise sources that are proportional to signal or time. Methods exist so that these contributions can be reduced to sub-electron levels or quantified and modelled with sufficient accuracy to remove their effect from science images. This paper will concentrate on the electronic subset of the intrinsic class, and develop methods to eliminate the components of reset, Johnson, 1/f, quantization, and drift noise sources. These components are independent of signal and they influence all signals in a similar manner, including signal and time dependent noise sources such PRNU and dark current. Because of this, the electronic noise contribution effectively sets the lower limit of sensitivity by masking low level signals under the electronic noise component. These noise sources, with the possible exception of drift, produce noise that manifests itself as pixel-to-pixel variation. Individual noise sources add in quadrature to form a total noise power for a given system. The ideal CCD camera system would remove these noise components completely by reducing their combined amplitude to below one equivalent photon (i.e. sub-electron noise).

Consider the character of these electronic noise components. Reset noise (or KTC noise) is the ambiguity in the charge deposited into the reset well before signal is clocked in. It is caused by the reset ripple voltage and Johnson noise current of the reset FET resistance. This latter component is a thermal noise source in parallel with the reset node capacitance. The reset contribution, N_{rst} , can be expressed as

$$N_{rst} = [(kTCB)^{1/2} + CV_{ripple}] / q \quad (e- rms) \quad (2)$$

Where k = Boltzmann constant, T = temperature, C = the capacitance value of the reset node, B = bandwidth of system, V_{ripple} = rms reset ripple voltage, and q = electron charge.

Johnson noise has a characteristic 'white' frequency spectrum i.e. the noise power density for any unit bandwidth is constant from DC to infinity. This implies that the white noise component of any electronic system is

proportional to the bandwidth of the system, hence the inclusion of system bandwidth in the above equation. $1/f$ noise sources however, have a characteristic power that is proportional to current density and approximately inversely proportional to frequency. This implies that high frequency systems contain a lower noise component from this source. The detector output amplifier and all gain components within the signal conditioning chain contribute both Johnson and $1/f$ components. The Johnson noise component of a signal chain element is given by

$$N_{\text{johnson}} = (4RCkT/Gq)B^{1/2} \quad (\text{e- rms} / \sqrt{\text{Hz}}) \quad (3)$$

Where R is the signal path resistance, C = reset node capacitance, k = Boltzmann constant, T = temperature, G = signal gain, q = electron charge, and B is system bandwidth. A representative curve is shown in figure 5.

The origin of $1/f$ noise is not fully understood, however the component can be approximated by the empirical expression

$$N_{1/f} = GI^k B/F^a q \quad (\text{e- rms}) \quad (4)$$

Where G = gain of the element, I = current density in the conduction path, k = empirical constant close to 3, B = system bandwidth, F = pixel read rate, a = empirical constant close to 2 for semiconductors, q = electron charge. Figure 6 show a representative curve for $1/f$ noise power.

Quantization noise will be generated by camera systems where the conversion process of the analog signal to a digital value has a resolution of less than one half of one equivalent photon (e^-). This is most often the case where large dynamic range is required for sky fields containing bright objects. Since the conversion process has a limited dynamic range, usually 2^{16} codes, the least significant bit ends up representing multiple photons and the signal becomes under sampled. When this occurs the signal amplitude acquires a noise component equal to

$$N_{\text{adc}} = (C / Gq) (V_{\text{LSB}} / 12^{1/2}) \quad (\text{e- rms}) \quad (5)$$

Where C = reset node capacitance, G = overall signal gain, q = electron charge, and V_{LSB} = voltage equivalent of the least significant converter bit.

In addition to quantization error, gain and offset error associated with non-perfect signal path elements and data converters are additional, fixed signal error sources but do not contribute a time or signal dependent change except by drift as described next.

Drift is characterised by being proportional to the operating temperature of the system and has a time constant much greater than the other noise components. However, given large detector array sizes, the amplitude of this component can become significant in long read times. Indeed, signal degradation due to drift is a serious problem when coherent data is required, spanning for example, one or more complete nights of observation. Currently,

this contribution can only be removed by careful and frequent observations of standard metrics. Drift therefore may be modelled as

$$N_{\text{drift}} = (CV_{\text{drift}} \Delta t) / (Gq) \quad (\text{e- rms}) \quad (6)$$

Where C = reset node capacitance, V_{drift} = voltage drift per degree k, Δt = delta temperature change, G = overall signal gain, and q = electron charge.

Thus, a reasonable model for the inherent independent electronic noise component of any observation is given by

$$N_{\text{rd}} = (N_{\text{rst}}^2 + N_{\text{johnson}}^2 + N_{1/f}^2 + N_{\text{adc}}^2 + N_{\text{drift}}^2)^{1/2} \quad (\text{e- rms}) \quad (7)$$

3. NOISE REMOVAL

Currently operating CCD cameras are designed with a compromise between medium frequency (maximise pixel rate) systems demanded for large CCD arrays that require high bandwidth (i.e. white noise limited performance) and 'low noise', low frequency low pass signal averaging systems dominated by 1/f noise. The classical method of CCD signal conditioning to eliminate noise components is to use a technique called correlated double sampling (CDS). This technique employs an integrator or low pass filter to integrate equal samples of the reset and signal values and derive an amplified difference signal. This technique is very effective in removing reset and 1/f components, however, the high frequency roll-off of the filter formed by the CDS integrator is determined by the pixel rate required. The high pixel rates that are now demanded means that the choice of electronic components fast enough to accommodate the signal accurately becomes critical. This generally results in pushing the system bandwidth (or acceptance) out wider than desired and allowing white noise components to become dominant. Figure 7 shows the bandwidth a typical CDS controller as a function of pixel rate.

The proposed technique addresses these problems by replacing the classic analog signal conditioning electronics with a software CDS thus reducing the complexity of analog circuitry in the front end. The front end will have a wide signal bandwidth and allow a very high analog to digital sample rate to be sustained on the signal. The analog signal conditioning is limited to a fixed gain stage, level shift, and anti-alias filtering to the Nyquist frequency determined by the sample rate. The sample rate will be in the order of 80 mega-samples / sec. The processing of this over-sampled signal is then done with firmware in a digital signal processor. The advantages of this technique are

1. Once the signal is sampled, no noise is added by the signal processing.
2. Much simpler analog processing allowing easier drift compensation.
3. Conversion gain of system (e- / ADU) independent of readout speed.
4. Digital signal processing allows much tighter control of signal processing design.

The combined application of these advantages is expected to allow the intrinsic electronic noise component to be reduced to below the equivalent one-photon level, leaving the signal and signal dependent noise components

available to the user. This is achieved by reducing elements contributing noise, stabilising the signal chain, and limiting the bandwidth to the minimum required to extract and process the signal.

Figures 8 to 14 illustrate the bandwidth of the CDS method (green trace) and compares this with the classical clamp and sample method (red trace) for given pixel rates of 70K to 1600K pixels / sec. In addition, the acceptance bandwidth of the proposed method (over sampling) is shown (blue trace). It can be seen that as pixel rates increase, the bandwidth that the CDS method 'sees' becomes more open with overall noise going up for a given noise density from the detector. In contrast, the proposed method functions as a filter that becomes sharper and with the side lobes occurring outside the limiting Nyquist bandwidth of the signal. Under these conditions, the proposed method 'sees' less bandwidth and hence the noise goes down for a given noise density.

The reduction of bandwidth associated with the 'over sampling' method is directly responsible for the reduction in noise seen in the acquisition process. In addition, the over sample method provides multiple data points for each sampled signal allowing further noise reduction to be obtained by averaging (or decimation). The additional noise reduction affects the white noise component which is cancelled by the root of the number of data points. The number of data points improves quantization error noise proportionally. This improvement is affected by the dither of the signal due to noise about its mean value during sampling. This process effectively removes the dynamic non-linearity of the converter and improves the resolution of the measurement.

Table 1 shows the predicted noise figures for the discussed readout schemes at different pixel rates. The noise values are scalars that when multiplied by the voltage equivalent of 1 electron at the detector output and divided by the noise voltage / root hertz of the detector will give values in electrons. The additional noise reductions applicable for the over sample method are not included in this table (i.e. further reductions are possible using decimation and filtering functions aside from those calculated here).

Readout Speed	Clamp / Sample	CDS	Over Sample
70,000 pix/sec	7.39	3.34	5.07
100,000 pix/sec	7.39	3.94	5.12
250,000 pix/sec	7.37	5.93	5.07
500,000 pix/sec	7.64	7.91	5.40
750,000 pix/sec	7.71	9.24	4.87
1,000,000 pix/sec	8.29	10.23	5.26
1,600,000 pix/sec	8.67	11.85	7.35

Table 1 Modelled prediction of noise performance for three readout schemes.

Notice that the over sample method noise reduction 'peaks' at around 750K pixels / sec. This is achieved by programming the number of samples and the aperture time that is used (In this case, 4 samples with 1/8th the pixel period).

The actual filter shape can be adjusted and optimised to best accommodate the desired pixel rate.

It is only recently that the technology has become available to realise this technique. Even so, the fast, high-resolution analog to digital converters that are required by this technique will need to be built from lower resolution sub components now available commercially. In addition to the analytic study, a simulation model has been built to further test the concept. Details and results of this simulation are contained within appendix A.

4. PHYSICAL IMPLEMENTATION

The over sampling technique can be implemented so as to relate to existing ING and SDSU CCD controller architectures. This will result in a board level change to the existing equipment to bring this novel concept into operational use. This has the following advantages

1. The technique can be introduced in a step-by-step manner with minimum disruption to existing equipment.
2. The technique can be retrofitted to only those cameras that will benefit most from noise free observing, thus reducing cost.
3. There will always be a fallback option if problems occur to the new equipment.
4. The technique can be offered as a retrofit option to other users of the same equipment.

5. EXPECTED PERFORMANCE

Characteristic	Value	Units
Signal channels per board	2	
Max readout speed per channel	1.5	Mpix / sec.
Conversion gain	1	e ⁻ / ADU.
Conversion dynamic range	2 ¹⁸	e ⁻
Fixed gain steps	1,2,4	e ⁻ / ADU
Board noise contribution	0	e ⁻
Combined detector / board electronic noise	< 1	e ⁻
Differential non linearity	< 0.5	e ⁻
Integral non linearity	< 1	e ⁻
Gain drift	0	e ⁻ 0 < t < 35C
Offset drift	< 2	e ⁻ 0 < t < 35C

6. DESIGN IMPLEMENTATION.

Fig 15 shows the basic architecture of a design to implement the described technique. The output of the CCD amplifier is resistively loaded to -5 volts to allow sufficient headroom for the difference amp and provide an independent quiet supply for the substrate reference. A D/A converter provides a DC voltage to subtract the mean reset voltage of the CCD amplifier output. This is summed to the signal before the difference amplifier buffering the CCD output signal to the second fixed gain stages. The difference amp provides pre-amplification of the signal plus common mode rejection and impedance

matching to the dc coupled second stage gain section. It also sets the overall sensitivity at $\frac{1}{2} e^-$ for the system. The signal is now presented to the low and high order stages where conversion to a digital value takes place. The low order stage samples the signal with full dynamic range once upon the convert command from the sequencer, usually after reset settling time. The nominal resolution of this conversion is $32 e^-$ based on an 18 bit dynamic range for the system. The value thus obtained is fed back to a 12 bit D / A such as to eliminate the gross offset measured by the low order stage and bringing the high order gain stage into range which is then unclamped and allowed to follow the high resolution signal. This signal is then sampled by a very fast (80 Msample / sec.) 8 bit converter. The static resolution of this stage provides $0.5 e^-$, however, since the noise rides on the converter, the quantization noise is reduced considerably as the noise dithers the converter input over many codes. In this way the high order stage reduces quantization noise and dynamic non-linearity errors of the converter by using the noise component to advantage. In addition the signal is sampled many times in the available pixel reset and video periods. These samples are fed to an on board DSP running firmware to filter the data, control the digitalisation process and emulate the original camera hardware behaviour. The signal reconstruction takes place within the DSP by summing the normalised values of the low and high order samples to form an 18-bit sum. This requires that we drop one bit from each conversion stage thus bringing the linearity to within $0.5 e^-$ across the static dynamic range of the converters. The multiple samples from each sampling period (reset and video) are then stacked to form an average value whose Johnson (white) noise component is reduced by the root of the stack depth. At this point further filtering can be applied if the amount of samples is low or low frequency components (ring / droop) make this necessary. The signal from the reset samples is then subtracted from the video sample to remove reset bias and remaining $1/f$ components. Finally the 18-bit result is truncated to present a 16-bit sample that is compatible to the camera system and contains the required dynamic range and resolution. The low component count and simple analog section design will reduce drift components to insignificant levels.

7. COSTS AND TIME SCALES

Task or Process	Labour time	Contract Costs	Part costs	
HW design	6 wk			
SW design	6 wk			
SW simulation	2 wk			
HW prototype	3 wk		5k	
HW layout		2k		
Manufacture		2k	0.5k	
Testing & characterisation	2 wk			
Documentation	1 wk			
TOTALS	20 wks	4k	5.5k	20 weeks - 9.5k£

Table 2 Estimated costs to produce one system

8. FIGURES

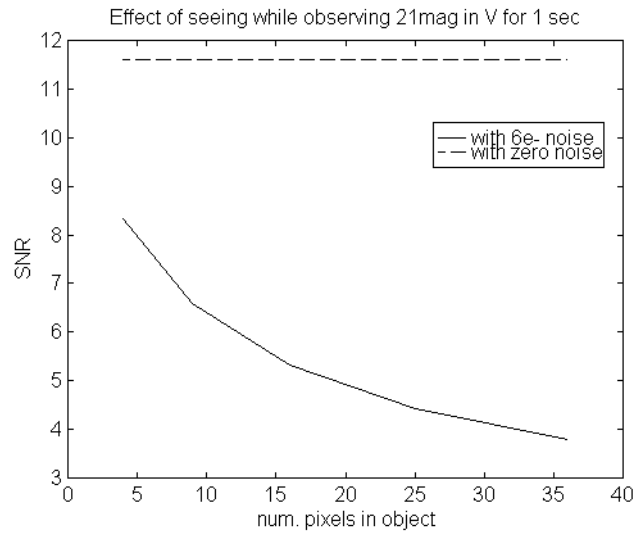


Fig 1. Effect of seeing on SNR.

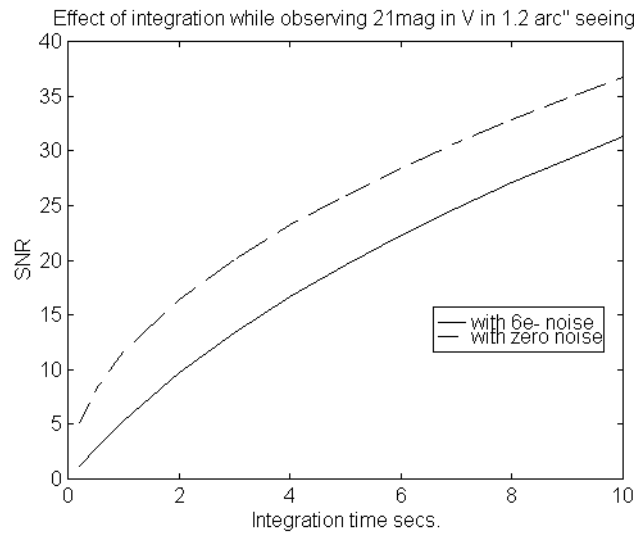


Fig 2. Effect of Integration time on SNR.

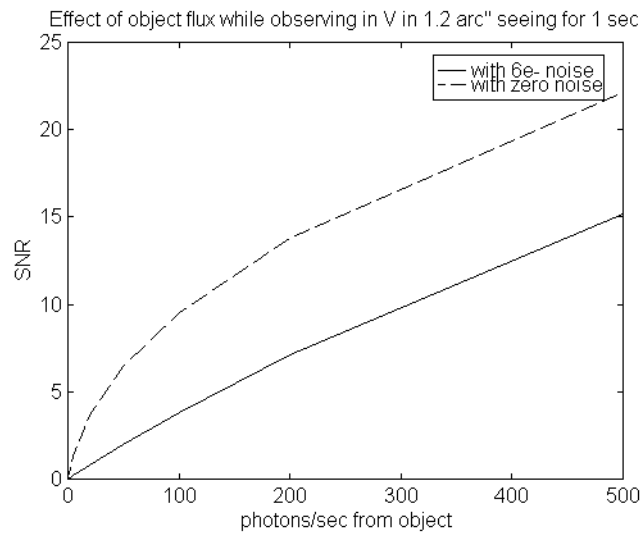


Fig 3. Effect of Object photon flux on SNR.

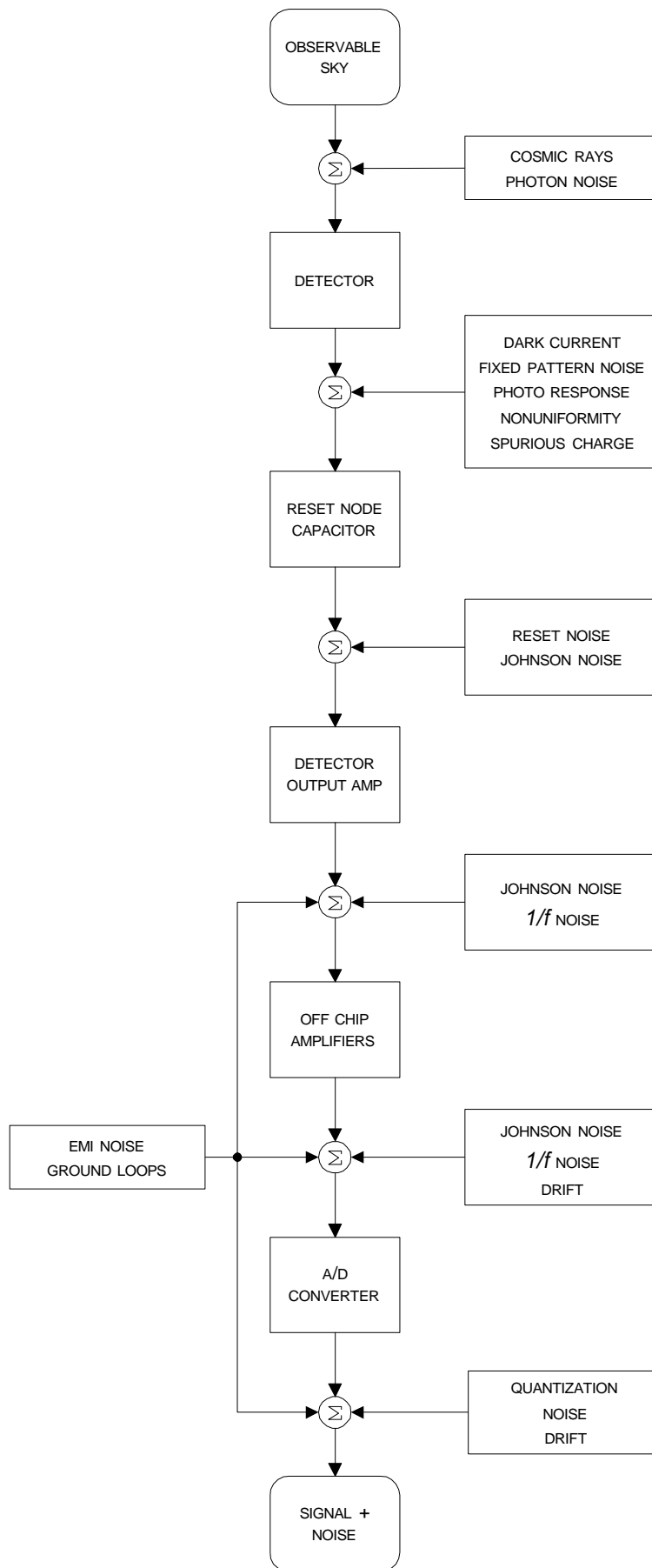


Fig 4. Noise source model for CCD Camera system

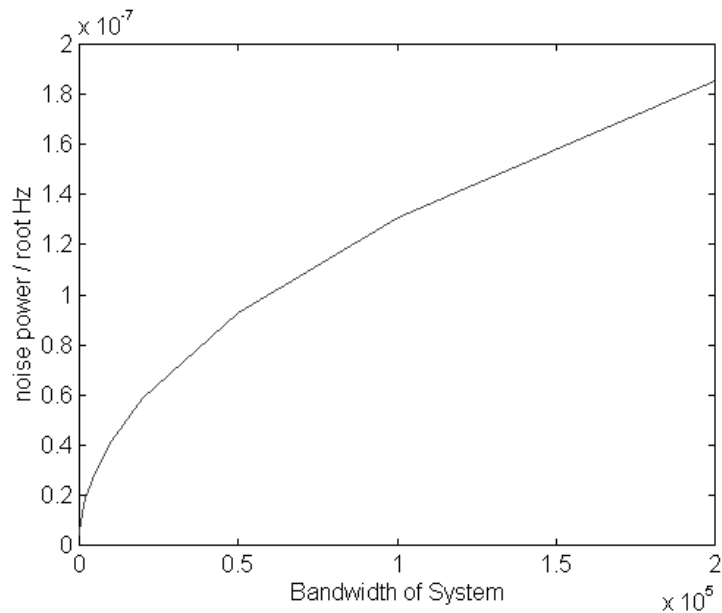


Fig 5. Johnson noise component as a function of system bandwidth.

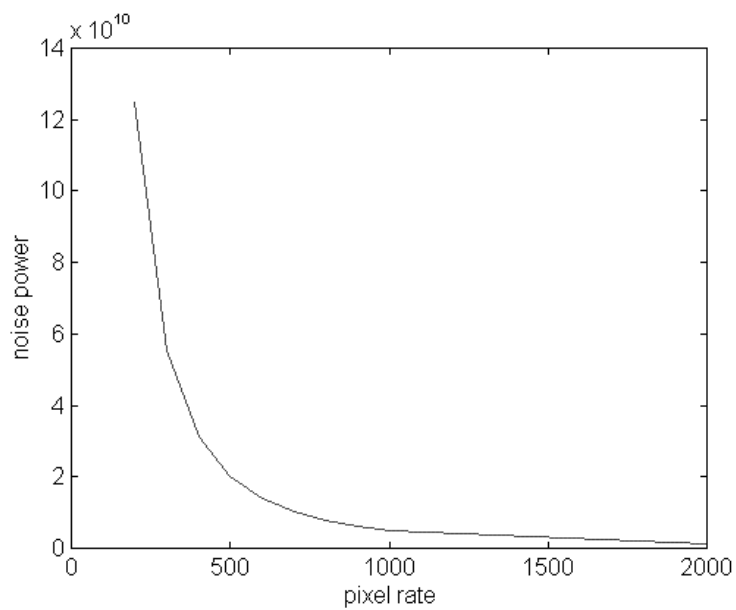


Fig 6. 1/f noise component as a function of pixel read rate.

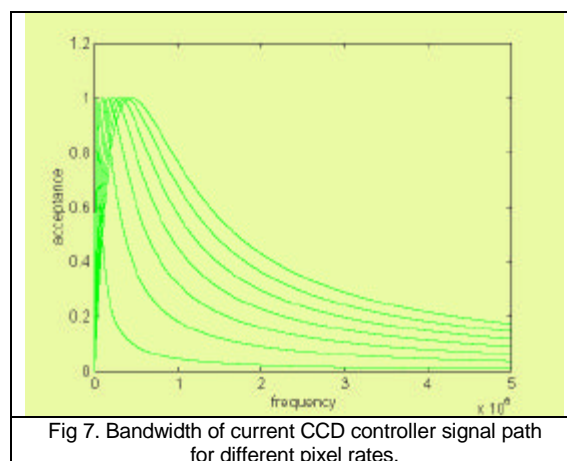


Fig 7. Bandwidth of current CCD controller signal path for different pixel rates.

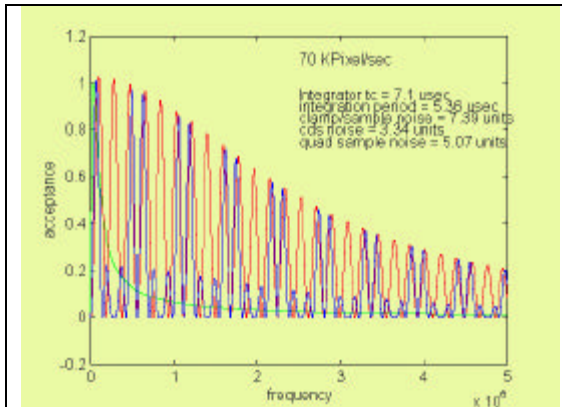


Fig 8. Comparison of system bandwidth at 70,000 pixels per sec.

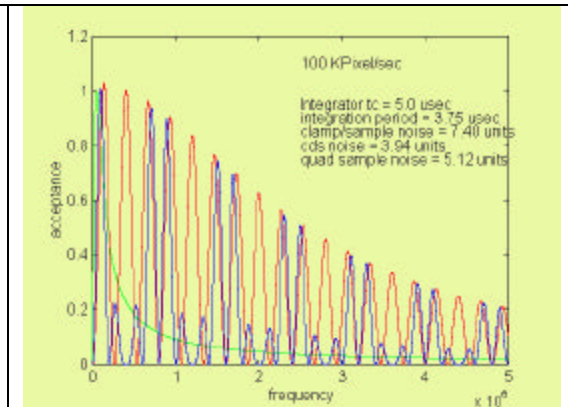


Fig 9. Comparison of system bandwidth at 100,000 pixels per sec.

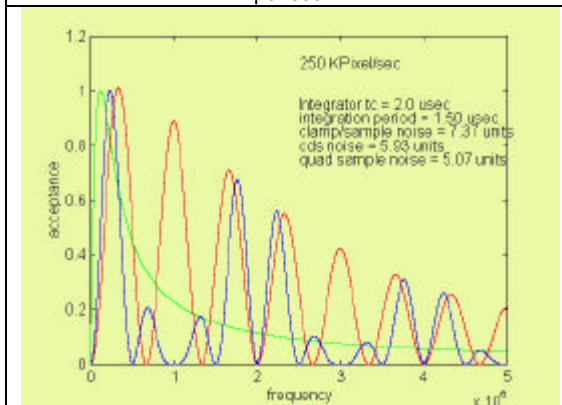


Fig 10. Comparison of system bandwidth at 250,000 pixels per sec.

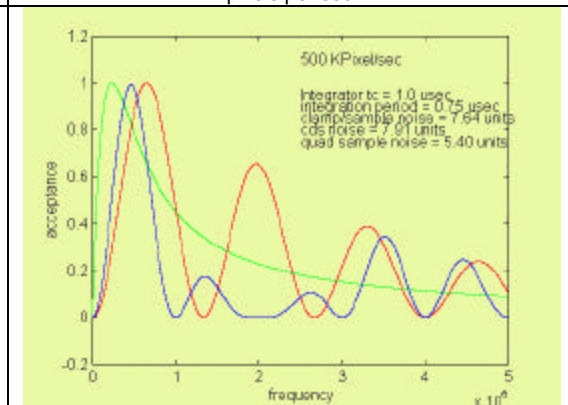


Fig 11. Comparison of system bandwidth at 500,000 pixels per sec.

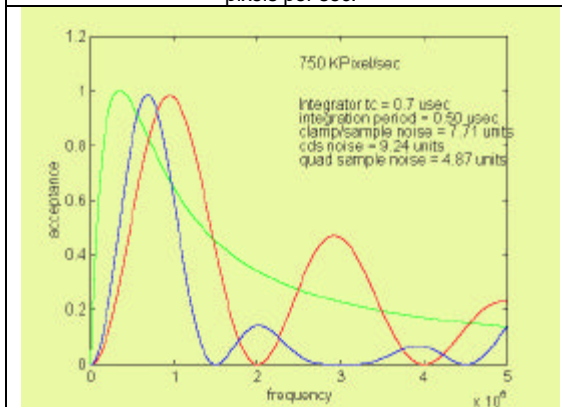


Fig 12. Comparison of system bandwidth at 750,000 pixels per sec.

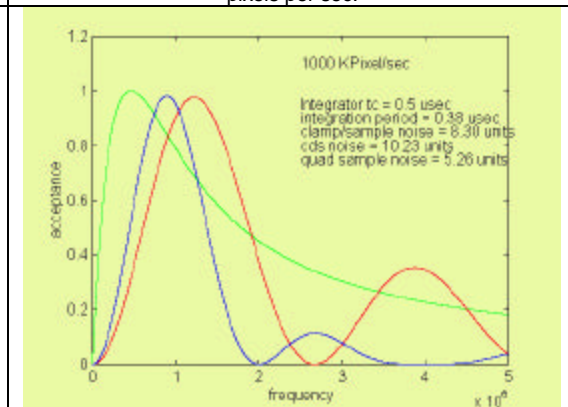


Fig 13. Comparison of system bandwidth at 1000,000 pixels per sec.

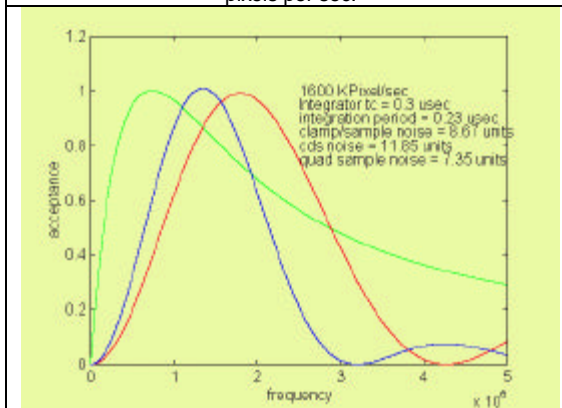


Fig 14. Comparison of system bandwidth at 1600,000 pixels per sec.

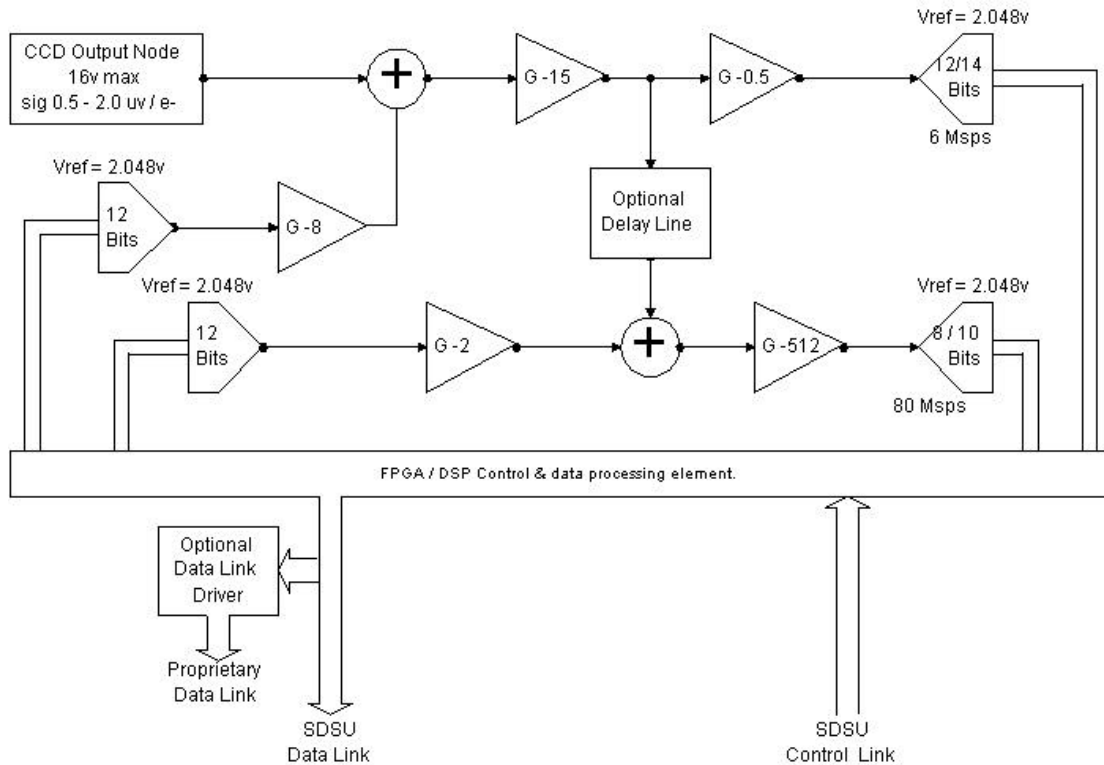


Fig 15. Over sampling concept model (One channel shown).

9. REFERENCES

- (1) J.R. Allington-Smith & H.E. Schwarz (1984)
Image photon detectors for optical astronomy
- (2) James Janesick, Tom Elliot
History and advancements of large area array scientific CCD imagers.
- (3) Gerald C. Holst
CCD arrays cameras and displays.
- (4) Prof. D.A. Bell
Noise in electronic systems.
- (5) James W. Beletic & Paola Amico
Optical detectors for astronomy conference.
Roger M. Smith.
Readout Speed Optimisation for Conventional Ccd's.
Ricardo E. Schmidt.
On the Optimization of CCD Readout Noise.
- (6) Tim J. Sobering.
KTC Noise and correlated double sampling.
- (7) Johannes Solhusvik, Frederic Dosiere, Jean Farre
Low noise CCD signal acquisition.
- (8) Tim Hardy, et. al.
CCD World email correspondence.

Appendix A.

Model to simulate the over sample method of signal acquisition.

A simulation package was written in MatLab to further test the concept of this scheme. The model contains 4 modules which correspond to the following areas of simulation.

1. Detector parameter file containing the characteristics of a simulated CCD.
2. Hardware parameter file containing the characteristics of proposed video processing chain.
3. Signal generator that produced a representative number of pixels with noise sources characterised by the detector parameters.
4. Sampling process which represented the hardware parameters in operation and reduces the generated signal to pixel values measured in electrons after acquisition and processing.

Various simulations were performed using representative detector models and the results tabulated. These are presented in Fig. 1 and 2. In addition, the output generated by a 1 Mpixel / sec readout of 10 pixels in an EEV42 device are shown in Figures 3 - 6. MatLab sources are available upon request. The simulation results presented here use the following noise values.

Case 1: Detector sensitivity = 4.5 μ volt / e-.

Johnson Noise = 13.5 μ volt rms. (3e- equivalent).

1 / f Noise = 20 μ volt @ 0Hz.

Reset Ripple = 1 millivolt rms.

Case 2: Detector sensitivity = 4.5 μ volt / e-.

Johnson Noise = 27 μ volt rms. (6e- equivalent).

1 / f Noise = 20 μ volt @ 0Hz.

Reset Ripple = 1 millivolt rms.

Case 3: Detector sensitivity = 4.5 μ volt / e-.

Johnson Noise = 27 μ volt rms. (6e- equivalent).

1 / f Noise = 40 μ volt @ 0Hz.

Reset Ripple = 1 millivolt rms.

Case 4: Detector sensitivity = 4.5 μ volt / e-.

Johnson Noise = 27 μ volt rms. (6e- equivalent).

1 / f Noise = 40 μ volt @ 0Hz.

Reset Ripple = 3 millivolt rms.

Sample Rate	Case 1	Case 2	Case 3	Case 4
500 KPix/sec.	0.50 e- rms.	1.00 e- rms.	0.74 e- rms.	0.89 e- rms.
1 MPix/sec.	0.78 e- rms.	2.15 e- rms.	1.67 e- rms.	1.60 e- rms.

Fig 1. Noise values for 40 Msps over sample simulation.

Sample Rate	Case 1	Case 2	Case 3	Case 4
500 KPix/sec.	0.46 e- rms.	0.99 e- rms.	0.39 e- rms.	0.60 e- rms.
1 MPix/sec.	0.96 e- rms.	2.24 e- rms.	1.08 e- rms.	1.18 e- rms.

Fig 2. Noise values for 80 Msps over sample simulation.

Data synthesis rate is 160.00 MHz
 Pixel readout is 1000000 Pix/Sec.
 Pixels are simulated with 12.00 e- signal
 Clock Feedthru is simulated with 0.500 volts amplitude.
 Johnson noise is present at 16.0 microvolts rms.
 1/f noise is present at 100.0 microvolts / root Hz.
 Reset noise is present at 3000.0 microvolts rms. at fundamental F = 60 KHz.
 Signal data saved as C:\matlab\nfccd\Nsig_2.m
 Johnson noise data saved as C:\matlab\nfccd\NJohn_2.m
 1/f noise data saved as C:\matlab\nfccd\Noof_2.m
 Conversion factor for this profile is 1.201 e- / ADU
 Coarse D/A adjustment set to 11.952 volts

Pixel data stats mean = 11.97 e-
 stdev = 0.84 e-
 maximum = 13.42 e-
 minimum = 10.58 e-Done.

Fig 3. Text output of simulation program.

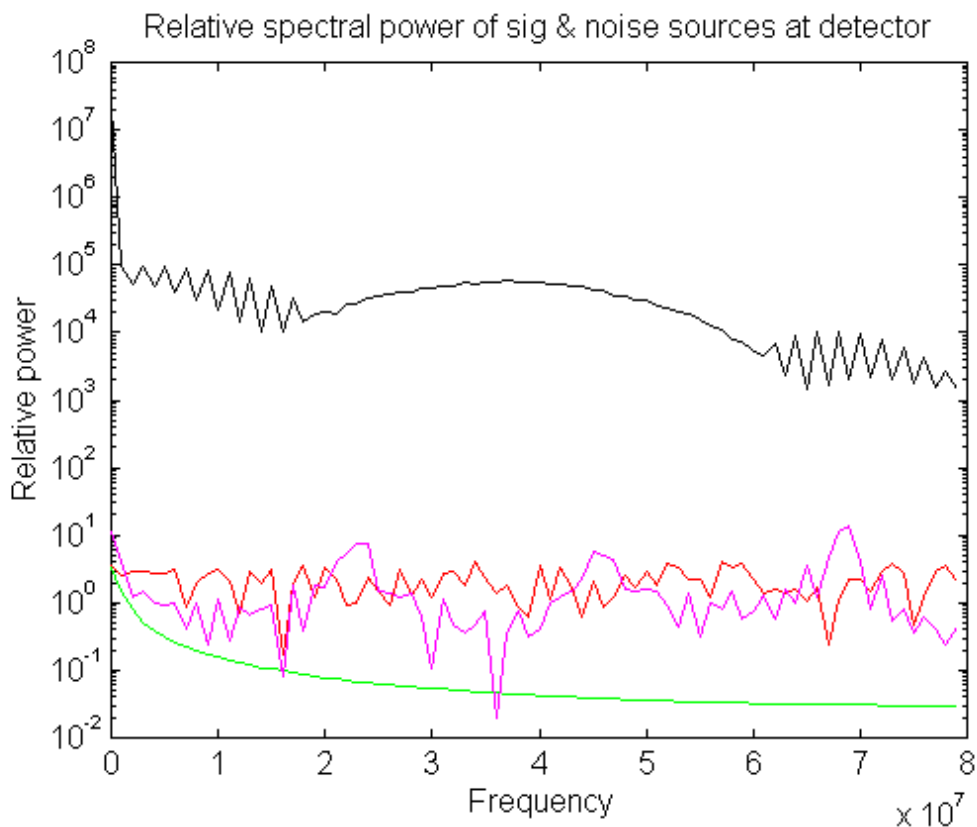


Fig 4. Relative power for reset, Johnson, signal and 1/f sources.

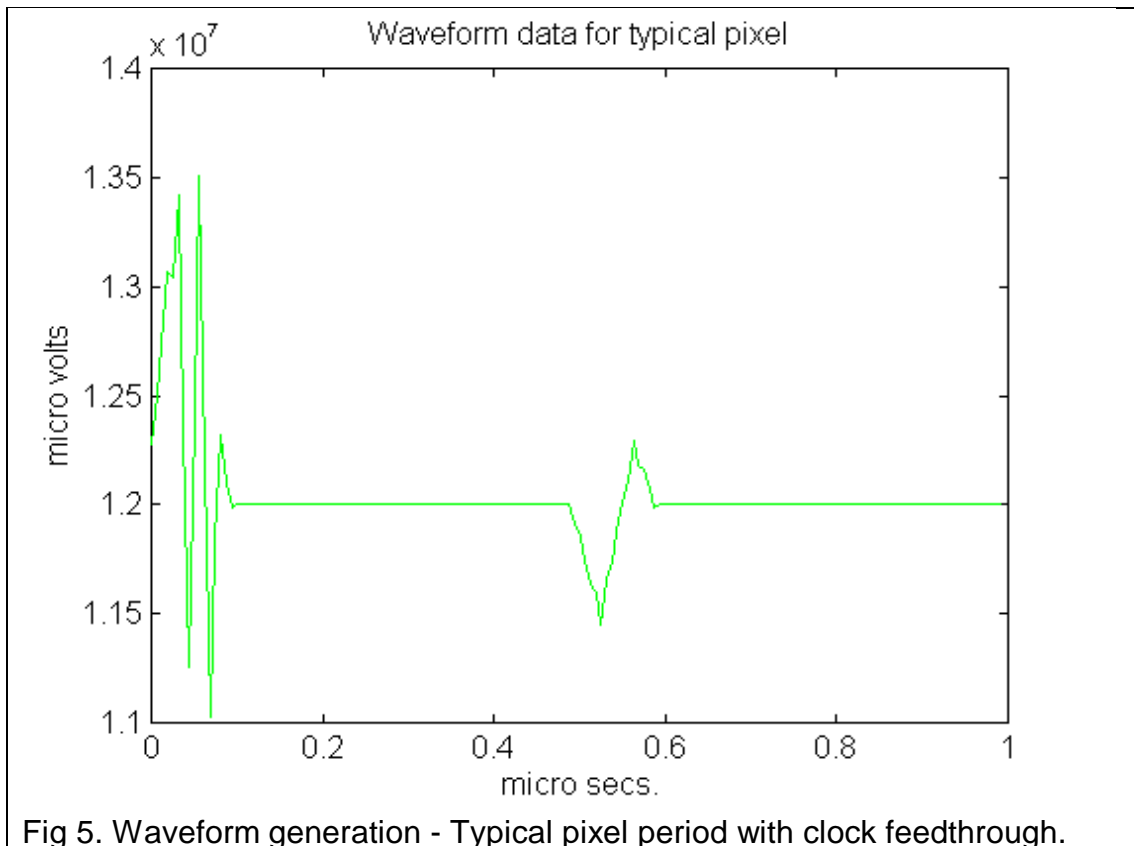


Fig 5. Waveform generation - Typical pixel period with clock feedthrough.

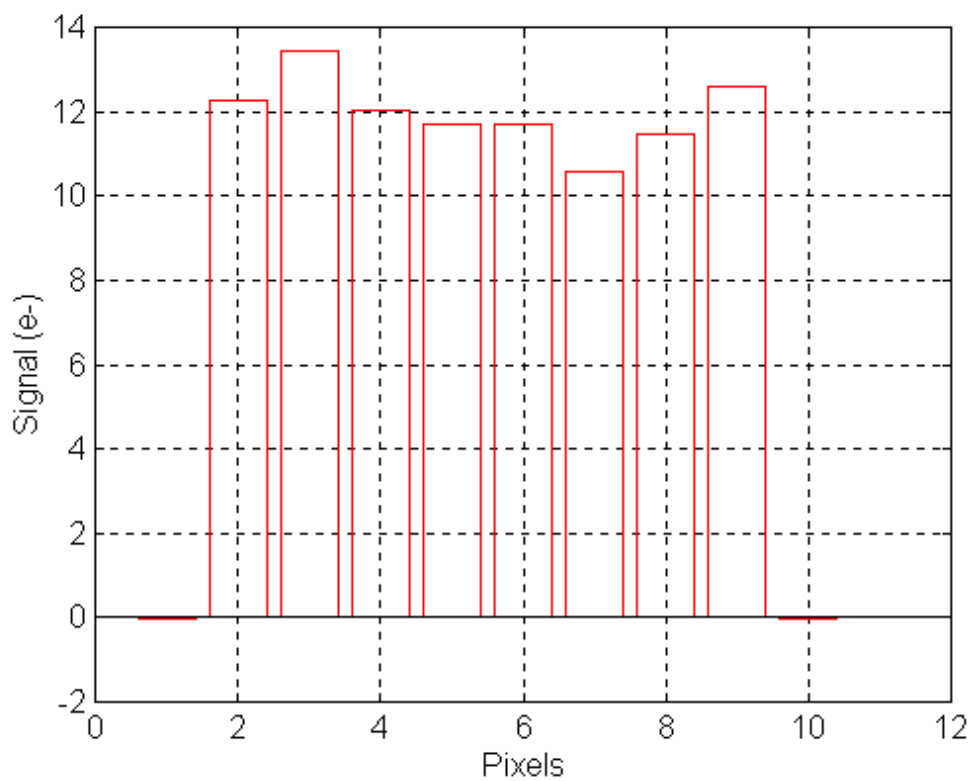


Fig 6. Simulation output for 10 pixels with nominal 12e- charge.